Counterintuitive thermo-optical response of metal-dielectric nanocomposite materials as a result of local electromagnetic field enhancement

Majid Rashidi-Huyeh and Bruno Palpant*
Institut des Nano-Sciences de Paris, Université Pierre et Marie Curie—Paris 6, Centre National de la Recherche Scientifique, Université Denis Diderot—Paris 7, 140 rue de Lourmel, 75015 Paris, France
(Received 23 December 2005; revised manuscript received 30 June 2006; published 4 August 2006)

Thermo-optical properties of composite materials consisting of noble metal nanoparticles spread in a dielectric host matrix are relevant for various fields in fundamental and applied nanosciences. We present a calculation of these properties in the framework of the Maxwell-Garnett effective medium model, exemplified by the case of gold nanoparticles in silica. The spectral variations of bulk gold thermo-optical coefficients, including implicitly the temperature dependence of intra- and interband transitions, are first extracted from experimental results of the literature. The composite material effective thermo-optical coefficients are then determined, accounting also for particle and matrix volume thermal expansion as well as temperature dependence of the matrix refractive index. These calculations lead to counterintuitive results in the vicinity of the surface plasmon resonance of the nanoparticles, originating from the local electromagnetic field enhancement. The findings are used to simulate the temperature dependence of the optical absorption spectrum of a Au:glass composite material. The result is compared with experimental data from the literature with good agreement.

DOI: 10.1103/PhysRevB.74.075405 PACS number(s): 78.67.Bf, 73.22.Lp, 78.20.Nv

I. INTRODUCTION

The fascinating optical properties of noble metal nanoparticles have recently led to many developments in different fundamental and applied fields such as ultrafast dynamics, surface-enhanced Raman scattering, near-field spectroscopy, nonlinear optics, industrial painting, study of ancient decorative art and craft techniques, photovoltaic device improvement, cancer therapy, chemical or biological sensor design, biological cell labeling, etc. The properties on which these developments lie are linked with the local electromagnetic field enhancement at the surface plasmon resonance (SPR) of the particles. This manifestation of confinement results, as often, in a response of the divided metal very different from the one of the bulk metal. While the optical response of materials containing metal nanoparticles has been and is still widely investigated, thermal properties remain much less studied. They represent, however, a relevant issue from the points of view of both fundamental physics and technological, or even medical, applications.[1–3] Parallel to pure thermal or thermodynamical properties of such materials,[4–8] their thermo-optical response has important involvements, for instance, in ultrafast electron dynamics and nonlinear optics. By *thermo-optical response* of a medium one usually designs the dependence of its complex optical properties (refraction and absorption of light) on temperature. This dependence is characterized by two thermo-optical coefficients, which denote the variation rate of the refractive index and extinction coefficient with T. In pump-probe experiments using femtosecond laser pulses, the signal observed after a few picosecond delay from the excitation (that is, once reached the thermal equilibrium between electrons and phonons in the particle) depends on the medium thermo-optical properties for both its sign and amplitude.[9–12] The thermo-optical behavior of a material also compete with its nonlinear optical response when using long-lasting laser pulses (generation of a thermal lensing effect).[13–16] It appears then particularly relevant to address such properties.

The rough first approach, when dealing with a medium consisting of an inhomogeneous mixture of different constituents, is to identify its global macroscopic properties with the volume average of the properties of each constituent, provided that the effect of the interaction between them can be neglected. In the present case, the thermo-optical coefficients of the nanocomposite medium could then be estimated as the volume average of the metal and dielectric ones. The validity of this crude approach will be addressed in the following. Some authors have already established analytical models to describe the temperature dependence of the optical constants of nanocomposite material, by accounting for some of the mechanisms involved.[17–19] The usual approach consists in considering the influence of temperature on the parameters of the Drude theory for the particle quasifree conduction electrons. Additional effects as thermal expansion of metal particle and host medium have sometimes been considered as well.

In the present paper, measurement results of bulk gold optical properties as a function of temperature, previously reported in the literature, are accurately analyzed in order to extract the thermo-optical coefficients of gold. The effective dielectric function given by the Maxwell-Garnett model is then derived relative to T, leading to the effective thermo-optical coefficients of the inhomogeneous medium. This calculation includes volume thermal expansion of both metal and surrounding medium as well as surrounding medium thermo-optical coefficient. It is illustrated in the case of gold nanoparticles embedded in a silica matrix. The role of the local electromagnetic field enhancement in the SPR spectral domain is then highlighted. The evolution of the absorption spectrum with increasing T is simulated and compared with other theoretical approaches and experimental results published in the literature. The reduction of lattice thermal expansion in metal particles constrained by a solid host matrix is finally deduced from this comparison.

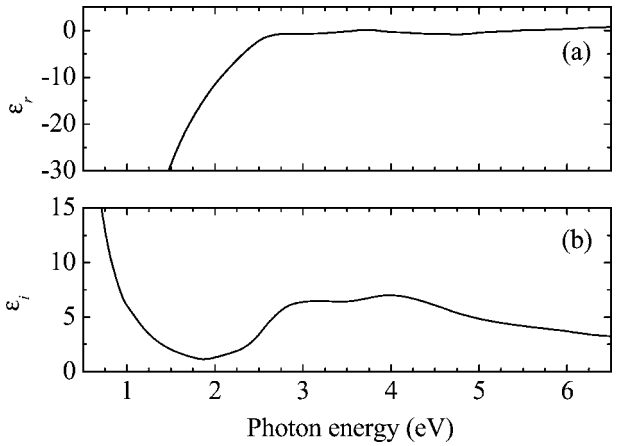

FIG. 1. Real (a) and imaginary (b) parts of gold dielectric function, as extracted from the experimental values of Ref. 34 further interpolated by spline-type curves.

II. GOLD THERMO-OPTICAL PROPERTIES

A. Dielectric function of gold

The optical response of a material is characterized by its complex index $\tilde{n}=n+i\kappa$ or its dielectric function $\tilde{\varepsilon}=\varepsilon_r+i\varepsilon_i=\tilde{n}^2$. n is the refractive index and κ the extinction coefficient. For sake of clarity, the frequency dependence of the different optical parameters will be often omitted in the following. The optical constants of the noble metals, and among them especially gold, have been studied both theoretically and experimentally by many groups in the sixties and seventies,[20–32] or even more recently.[33] In these works the different possible mechanisms responsible for the metal optical properties have been assessed. These properties fundamentally originate from the contributions of both intraband and interband electronic transitions. The former represent transitions within the conduction band while the latter correspond to transitions from bound levels (d bands in noble metals in the visible spectral domain) to the conduction band above the Fermi level. The intraband contribution to the metal dielectric function, given by the Drude theory for quasifree electrons, writes

$$\tilde{\varepsilon}^{intra}(\omega) = 1 - \frac{\omega_p^2}{\omega(\omega + i\gamma)}, \tag{1}$$

where γ is a phenomenological damping constant which is inversely proportional to the electron mean free path and $\omega_p=(4\pi Ne^2/m^*)^{1/2}$ is the volume plasma frequency (N, e, and m^* are the conduction electron density, electric charge, and effective mass, respectively). The spectral variations of the real and imaginary parts of the gold dielectric function, as given in Ref. 34, are presented in Fig. 1. In the red and infrared (IR) spectral zones ($E<2$ eV, where E is the photon energy) the only possible transitions are the intraband ones and absorption (ε_i) decreases with increasing photon energy. Interband transitions are possible at higher E values. The interband absorption threshold energy is worth 1.84 eV (674 nm) at ambient temperature, corresponding to transitions from the d band to the Fermi level near the X point in the Brillouin zone (BZ).[25] There are two local maxima at 2.8 and 4.0 eV in ε_i, corresponding to interband transitions in the vicinity of different points of the BZ. It is worth noticing that the discrepancies between optical constant values observed from one work to another in the literature (of the order of 15% for the second absorption maximum at 4.0 eV) is attributed to various sample effects such as surface roughness, confinement, strain, etc.[25] It is also worth mentioning that an anomalous absorption, located between 1 and 2 eV, has sometimes been reported. Thèye suggested it to be related to some kind of defects or impurities in the samples,[21] while Hodgson attributed it to indirect transitions.[26]

B. Temperature dependence of gold optical constants

Many different effects can contribute to modify the optical properties of noble metals under temperature variation. They are schematically summarized in Fig. 2. The most important of these effects are: (i) Isotropic thermal expansion,

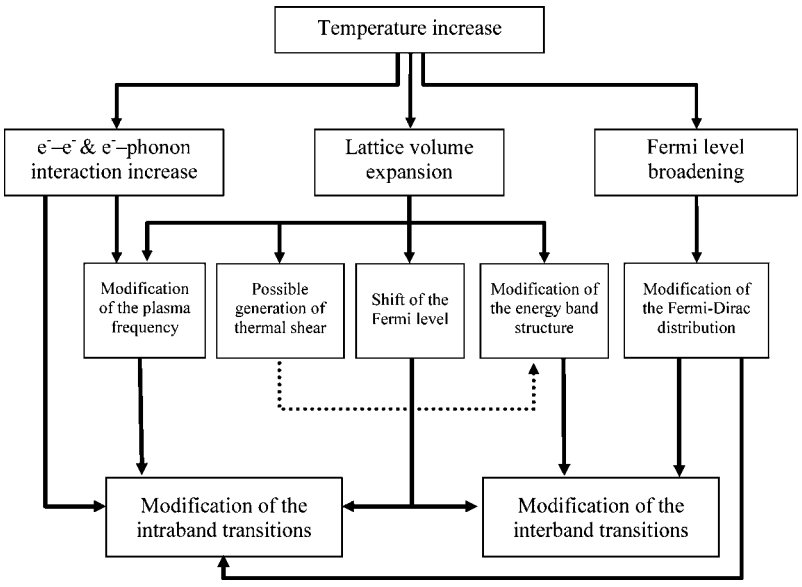

FIG. 2. Schematic representation of the different thermal effects which can lead to the modification of the optical properties of bulk noble metals.

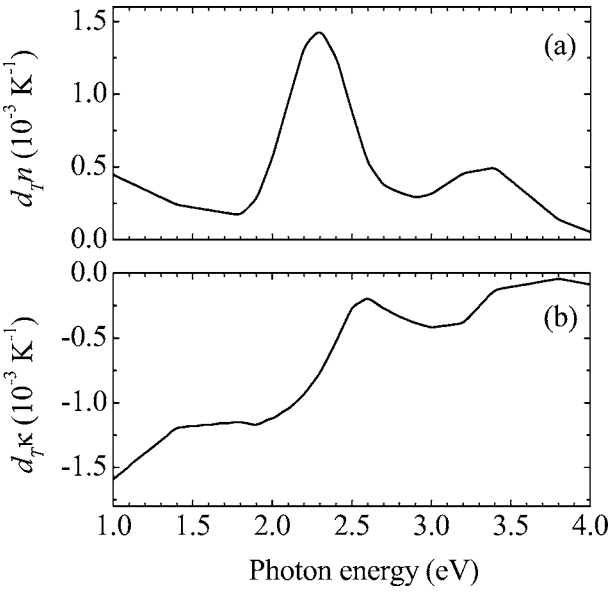

FIG. 3. Spectral variations of the thermo-optical coefficients $d_T n$ (a) and $d_T \kappa$ (b) of bulk gold (mean values over the temperature range from T=295 K to 670 K).

(ii) increase of electron-phonon and electron-electron scattering rates, (iii) broadening of the Fermi level.[27–30] Thermal dilatation causes the modification of the electron energy band structure (through interatomic distance), plasma frequency (through electron density), and Fermi energy. The second effect can change both relaxation time and plasma frequency, and the third one modifies the Fermi-Dirac distribution. All these phenomena can affect the interband and/or intraband transitions directly or indirectly. The contribution of each for a particular photon energy depends on temperature as well as on temperature variation.[28] The maximum thermal modulation of the optical properties of gold is situated around 2.4 eV, corresponding to the *d* band to Fermi-level transition near the *X* and *L* points of the BZ. Rosei *et al.* have theoretically studied the thermo-optical effect in gold through a model based on the interband transition thermal modulation near the *L* point of the BZ.[29,30] In addition, as the electron energy band structure and Fermi-Dirac distribution are modified with temperature, the interband absorption edge is also expected to depend on temperature. Winsemius *et al.* studied the thermal dependence of the gold interband absorption edge attributed to two transitions near the *X* and *L* points of the BZ.[31,32] Hodgson observed the increase with temperature of the slight anomalous absorption centered between 1 and 2 eV.[26]

The temperature dependence of the optical properties is characterized by the thermo-optical coefficients, i.e., the derivative of the refractive index and extinction coefficient relative to temperature, dn/dT and $d\kappa/dT$. In the following, the derivative of a variable x relative to T, dx/dT, will be rather written $d_T x$ for sake of clarity. Figure 3 presents the variations of the gold thermo-optical coefficients versus photon energy, extracted from Ref. 27 by using the following method. In Ref. 27 the spectral variations of gold absorption, described by ε_i/λ, are reported for five different temperatures T_j (j=1 to 5) from 295 K to 770 K. We calculate the real part of the dielectric function for each T_j as follows: (i) The imaginary part of the interband transition contribution, $\varepsilon_i^{inter}(\omega)$, is extracted from the imaginary part of the total dielectric function, $\varepsilon_i(\omega)$, by using the results of Refs. 31 and 32 where the interband absorption edge characteristics are measured as a function of temperature. (ii) Kramers-Kronig analysis is carried out to obtain the interband real part, $\varepsilon_r^{inter}(\omega)$, from $\varepsilon_i^{inter}(\omega)$. (iii) The intraband contribution is determined by using the Drude parameters given for different temperatures (from 295 K to 670 K) in Ref. 27. The authors obtained these parameters by fitting the real and imaginary parts of $\tilde{\varepsilon}(\omega)$ in the IR spectral domain with the quasifree electron model [Eq. (1)], since in this domain interband transitions do not occur, as stated above. γ then increases from 4.17×10^{13} s^{-1} to 1.04×10^{14} s^{-1} and $\hbar\omega_p$ from 9.28 eV to 9.48 eV when temperature increases from 295 K to 670 K.[27] On one hand, the increase of γ with T is not surprising since this damping constant accounts for the electron collision rate. On the other hand, the volume plasmon frequency exhibits a small rise with increasing T: The effect of the decrease of the electron density N with lattice expansion is slightly overtook by the effect of the decrease of the effective mass m^*. The spectra $n_j(\omega)$ and $\kappa_j(\omega)$ are then calculated at each temperature T_j from the values of $\tilde{\varepsilon}_j(\omega)$ obtained by the procedure described above.

Finally, assuming that n and κ vary roughly linearly with T within the temperature range under consideration (which has been verified), we calculate $d_T n$ (respectively $d_T \kappa$) at every photon energy from the slope of a linear fit to $n_j(T_j)$ [$\kappa_j(T_j)$]. When experiments are realized at two different temperatures T_1 and T_2 the quantity $\Delta\tilde{n}/\Delta T=[\tilde{n}(T_2)-\tilde{n}(T_1)]/(T_2-T_1)$ may be viewed as the estimated value of $d_T\tilde{n}$ at the average temperature $T_{av}=(T_1+T_2)/2$. Winsemius *et al.* have shown excellent agreement between the values of $\Delta\varepsilon_i/\Delta T$ deduced from experiments at two different temperatures and the ones measured at T_{av} by an optical thermomodulation method for both Au and Ag.[28] Our results regarding the spectral variations of the gold thermo-optical coefficients (Fig. 3) can then be considered as mean values within the temperature range from 295 K to 670 K. As can be observed on Fig. 3, heating of bulk gold leads to an increase of its refractive index ($d_T n>0$) and a decrease of its extinction coefficient ($d_T \kappa<0$). The maximum thermal sensitivity of the optical properties in the spectral domain displayed and temperature range under consideration lies around the interband transition threshold. The corresponding features on the spectra are superimposed on the variations due to the temperature dependence of the Drude parameters (collision rate, effective mass, and density of the conduction electrons), increasing from UV to IR.

III. VARIATIONS OF THE NANOCOMPOSITE MATERIAL OPTICAL RESPONSE WITH TEMPERATURE

A. Temperature dependence of the effective optical constants

We will now focus on the thermo-optical properties of inhomogeneous media consisting of noble metal nanoparticles spread in a transparent dielectric host. Such materials

have aroused much interest thanks to their original linear and non-linear optical properties related to the surface plasmon resonance (SPR) phenomenon. These properties are thought to evolve with temperature as the optical response of their constituents do. A naive way to account for the presence of both dielectric and metal in the medium would be to calculate the volume-weighted average value of the complex thermo-optical coefficient, $\langle d_T\tilde{n}\rangle_{vol}$, as

$$\langle d_T\tilde{n}\rangle_{vol} = p d_T\tilde{n} + (1-p) d_T n_m. \quad (2)$$

However, it will be shown in the following that this approach is, of course, fully improper, due to dielectric confinement effect in nanoparticles.

Among the numerous approaches which have been developed in order to describe the optical properties of inhomogeneous media, the pioneering Maxwell-Garnett one is surely the most simple.[35] It is suited for a medium consisting of spheres of material A spread in a host material B. The sphere radius is small enough to validate the use of the quasistatic approximation, and the volume filling fraction of A does not exceed about 15%. Let us mention here that any quantum confinement effect due to finite particle size will be disregarded in the present approach. Especially, the features originating from the SPR as predicted by the following calculations are expected to be damped and shifted as soon as particle diameter is reduced below a few nanometers. As every effective medium theory, the Maxwell-Garnett one aims at describing the effective optical constants of the whole medium as a function of those of its constituents. It is applied here for metal nanospheres (complex dielectric function $\tilde{\varepsilon}$) in a dielectric matrix (real refractive index $n_m = \varepsilon_m^{1/2}$). The inhomogeneous medium effective dielectric function, $\tilde{\varepsilon}_{eff}(\omega)$, then writes

$$\tilde{\varepsilon}_{eff} = \varepsilon_m \frac{\tilde{\varepsilon}(1+2p) + 2\varepsilon_m(1-p)}{\tilde{\varepsilon}(1-p) + \varepsilon_m(2+p)}, \quad (3)$$

where p is the metal volume fraction. We will illustrate the influence of temperature on the effective optical properties by examining the case of gold nanoparticles in a silica matrix ($Au:SiO_2$), probably the most widely studied metal/dielectric nanocomposite material. If the conditions ensuring the validity of the Maxwell-Garnett theory are fulfilled, then the value of the effective dielectric function at any specified temperature can be given by Eq. (3) provided the values of all the parameters involved are also taken at this temperature. The temperature dependence of the composite material optical properties ($d_T\tilde{n}_{eff} = d_T n_{eff} + i d_T\kappa_{eff}$) can then be derived from Eq. (3) through $d_T\tilde{\varepsilon}_{eff} = d_T(\tilde{n}_{eff}^2)$ without further restricting the requirements of the Maxwell-Garnett model. In fact, all three variables in this equation ($\tilde{\varepsilon}$, ε_m, and p) can vary with T. Let us now examine the corresponding contributions to $d_T\tilde{n}_{eff}$, that is, the terms proportional to d_Tp, d_Tn_m, and $d_T\tilde{n}$. First, metal nanoparticle lattice expansion under temperature rise tends to increase the metal volume fraction, whereas matrix thermal expansion tends to decrease it. If the gold and silica thermal dilatations are considered as independent processes occurring freely, that is without any strain

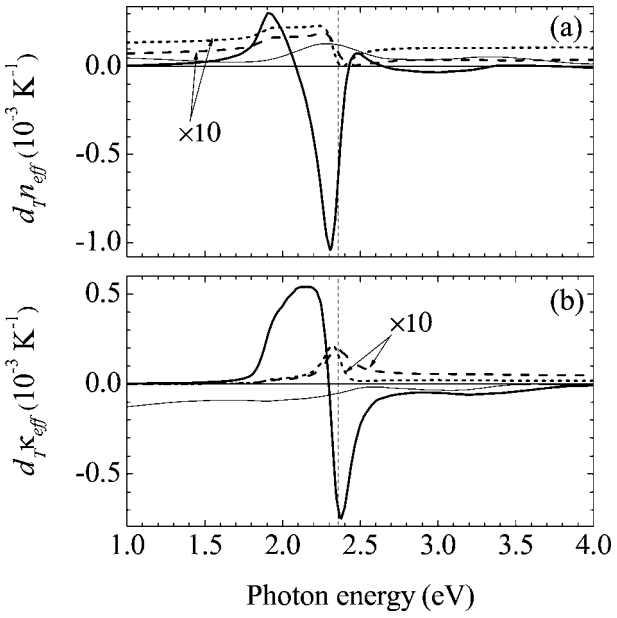

FIG. 4. Spectral variations of the different contributions to d_Tn_{eff} (a) and $d_T\kappa_{eff}$ (b) for a $Au:SiO_2$ nanocomposite material with $p=8\%$, calculated by deriving Maxwell-Garnett formula [Eq. (3)]. Thick solid line: contribution of the gold complex index temperature dependence (terms proportional to d_Tn and $d_T\kappa$); dashed line: contribution of the gold concentration temperature dependence (terms proportional to d_Tp); dotted line: contribution of the matrix index temperature dependence (terms proportional to d_Tn_m). The last two ones have been magnified ten times for sake of clarity. The "naive" thermo-optical coefficient spectra of the inhomogeneous medium, corresponding to the volume-weighted average of gold and silica ones, $d_T\tilde{n}'$ [Eq. (2)], have been added for comparison (thin solid line). The vertical dashed line denotes the position of the SPR maximum (2.36 eV), defined as the energy of the absorption coefficient maximum calculated at $T=400$ K.

generated at the interface, the concentration variation rate with temperature is given by

$$d_Tp = 3p(1-p)(\beta_{Au} - \beta_{SiO_2}), \quad (4)$$

where β_{Au} and β_{SiO_2} denote the thermal linear expansion coefficients of gold and silica, respectively. Let us underline that, as dilatation is actually not free and strain is generated at the particle/matrix interface, the expression above [Eq. (4)] overestimates the value of d_Tp. The thermal linear expansion coefficients of the constituents at ambient temperature are worth 14×10^{-6} K^{-1} for gold[36] and 0.5×10^{-6} K^{-1} for silica.[37] For a $Au:SiO_2$ material with $p=8\%$, Eq. (4) then provides $d_Tp = 3\times10^{-6}$ K^{-1}.

Second, the dielectric matrix thermorefractive coefficient, d_Tn_m, is worth about 1.5×10^{-5} K^{-1} within our spectral domain and temperature range, as given for instance in Ref. 38. Figure 4 reports the spectral profile of the different contributions to d_Tn_{eff} and $d_T\kappa_{eff}$ for $p=8\%$. Note that the contributions of the temperature dependence of both matrix index (terms proportional to d_Tn_m) and metal concentration (terms proportional to d_Tp) have been magnified ten times as compared with the contribution of gold index temperature depen-

dence (terms proportional to $d_T n$ and $d_T \kappa$) in order to improve the clarity of the figure. As can be observed, the thermo-optical contributions of matrix index and metal concentration are positive over the whole spectrum and present a resonance behavior close to the SPR (the maximum of which is located at 2.36 eV for $p=8\%$ and $T=400$ K). At this concentration value, these two contributions remain negligible as compared with the metal index one in the vicinity of the SPR. In this spectral range and for high enough p values (i.e., sufficient for the SPR band to appear in the linear absorption spectrum) the derivation of Eq. (3) then simplifies into the only thermo-optical contribution of the metal index

$$d_T\tilde{\varepsilon}_{eff} = \frac{9p\varepsilon_m^2}{[\tilde{\varepsilon}(1-p)+\varepsilon_m(2+p)]^2} d_T\tilde{\varepsilon}. \tag{5}$$

This dominant term exhibits strong amplitude and sign variations in both the effective refraction and extinction spectra around the SPR [see Figs. 4(a) and 4(b)]. The surprising fact is that, whereas the metal amount in the medium is relatively low, the effective thermo-optical response is completely different from the one of the main constituent, that is, the dielectric host medium. Indeed, the thermo-optical coefficient of the latter is low as compared with the absolute value of $d_T n_{eff}$ around the SPR. Moreover, whereas $d_T n_m$ is positive at ambient temperature over the visible spectrum, $d_T n_{eff}$ presents large negative values in the vicinity of the SPR maximum. This implies for instance that, even at low metal filling fraction, the thermal lensing effect in a nanocomposite material cannot be described by the only dielectric host thermo-optical properties as it has yet been done.[39,40] Moreover, an absorptive thermo-optical effect, which is always disregarded in the literature, can occur parallel to the refractive one. Of course, when p tends to zero, Eq. (5) is no more valid and $d_T n_{eff}$ and $d_T \kappa_{eff}$ converge to $d_T n_m$ and zero, respectively.

The curve corresponding to the naive volume-averaged estimation [Eq. (2)] is reported on Fig. 4 as a thin solid line. It can be observed that this simple approach gives results very different from those obtained through the optical effective medium one, not only regarding the amplitude of the coefficients, but also their spectral profile and their sign. Hence, what was inferred more than a century ago about the linear optical properties of an inhomogeneous medium[35] is also valid for its thermo-optical properties: The effective optical constants (respectively, thermo-optical coefficients) of the medium are not simply given by the volume average of those of its constituents. This fact, highlighted by the discrepancies between the thin and thick continuous curves on Fig. 4, is due to the complex electromagnetic field enhancement at the SPR of the metal nanoparticles. Such a "counterintuitive" result was already underlined by Smith *et al.* regarding the influence of the local field enhancement on the effective third-order nonlinear susceptibility of nanocomposite materials.[41] Here, the most spectacular realization of this effect lies probably in the light refraction properties: Whereas both gold and silica have a positive thermorefractive coefficient, the composite medium consisting of a heterogeneous mixing of gold and silica exhibits a large negative one around the SPR.

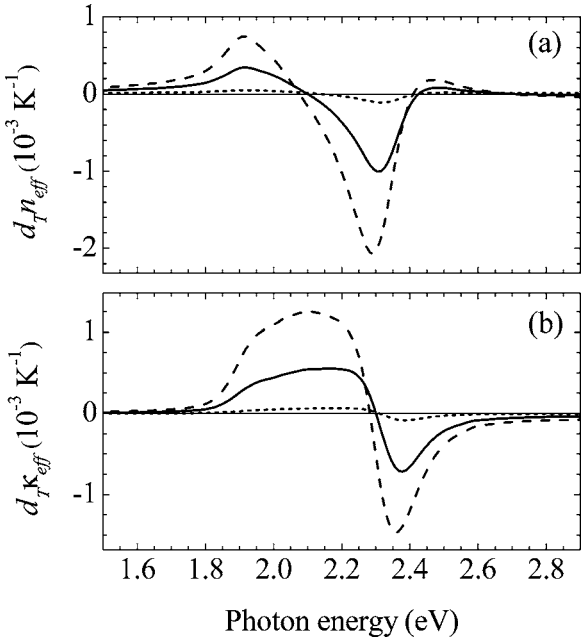

FIG. 5. Spectral variations of the effective thermo-optical coefficients $d_T n_{eff}$ (a) and $d_T \kappa_{eff}$ (b) of a Au:SiO_2 nanocomposite material for three different gold concentrations: $p=1\%$ (dotted line), $p=8\%$ (solid line), and $p=15\%$ (dashed line).

Such as the effective dielectric function [Eq. (3)], the effective complex thermo-optical coefficient [Eq. (5)] presents a resonant behavior around the estimated SPR circular frequency, Ω_{SPR}, defined by

$$\varepsilon_r(\Omega_{SPR}) = -\frac{2+p}{1-p}\varepsilon_m(\Omega_{SPR}). \tag{6}$$

The enhancement of the local electromagnetic field at resonance results in the enhancement of the thermo-optical response of the nanocomposite medium. However, due to the square in the denominator and the multiplication by the complex quantity $d_T\tilde{\varepsilon}$ [Eq. (5)], the effect of this enhancement on the spectral profile (sign, position, width) of $d_T n_{eff}$ and $d_T \kappa_{eff}$ is not straightforward.

Out of the SPR spectral range, the situation is quite different. One can observe on Fig. 4 that shifting to the infrared (photon energy less than ~1.5 eV) or to the ultraviolet (photon energy higher than ~3 eV) leads to the cancellation of the term proportional to $d_T\tilde{\varepsilon}$ in $d_T\tilde{\varepsilon}_{eff}$, while the relative weight of the terms proportional to $d_T n_m$ and $d_T p$ increase. This terms cannot be neglected any more, in particular in the refractive thermo-optical coefficient [Fig. 4(a)].

Let us examine the influence of metal concentration on the material thermo-optical properties. Figure 5 presents the spectral profiles of both $d_T n_{eff}$ and $d_T \kappa_{eff}$ for Au:SiO_2 with $p=1\%$, 8% and 15%. One can observe that, just as for the effective optical properties, the location of the thermo-optical features linked with the SPR (minimum of $d_T n_{eff}$ and $d_T \kappa_{eff}$ between 2.2 and 2.4 eV) shifts to lower photon energies as metal concentration increases.

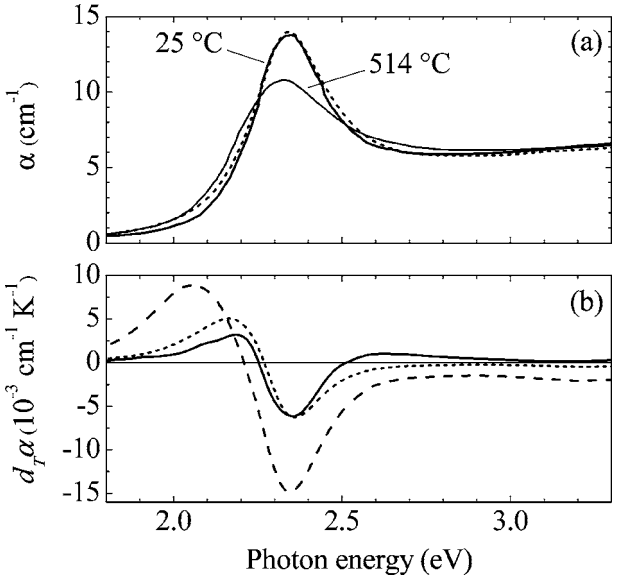

FIG. 6. (a) Spectral variations of the optical absorption, defined as $\alpha=2n\kappa/\lambda$, of glass-embedded gold nanoparticles (diameter: 12 nm), reported from the results of Doremus (Fig. 10 of Ref. 42) obtained at 25 °C (thick solid line) and 514 °C (thin solid line). The dotted line corresponds to the Maxwell-Garnett model calculation at ambient temperature [Eq. (3)] with fitted metal volume fraction $p=5.3\times10^{-5}$ and Drude collision factor $\gamma=0.23$ eV. (b) Thermo-optical absorption, $d_T\alpha$, derived from the experimental results of Doremus (solid line), calculated through our model assuming free metal thermal expansion (dotted line) and accounting for the reduced thermal expansion in matrix-embedded metal particles by quenching by an arbitrary factor 3 the contribution of metal thermo-optical coefficient, $d_T\tilde{\eta}$, to the effective medium one (dashed line).

B. Variation of the absorption spectrum with temperature

We will now apply the approach described above to the optical absorption spectrum of nanocomposite media. A few experimental works were reported in the literature regarding the evolution of absorption with temperature.[19,42–46] Doremus, for instance, measured the absorption spectrum of Au:glass composites at 25 °C and 514 °C.[42] His results regarding particles with a mean radius $R=6$ nm (Fig. 10 of Ref. 42) are reported in Fig. 6(a) (solid lines). The SPR band lies around ~2.35 eV. The monotonous absorption observed in the blue-UV range is due to interband transitions. As can be observed, the SPR band is broadened and damped with increasing temperature, and its maximum is shifted to lower energies. The broadening particularly occurs in the low-energy wing of the resonance band. For these material composition and temperature increase, the change in gold volume fraction is about 10^{-3} and cannot be directly responsible for the absorption peak shift. Thus, absorption shift is attributed to gold optical constant variations with temperature, "amplified" by the local field enhancement, as stated above. Doremus also measured similar behavior for smaller particles (2.5 nm diameter, see Fig. 12 of Ref. 42), even if the amplitude, width and location of the SPR band are modified by quantum size effects. The author ascribed the modification of the SPR band with increasing temperature to the decrease of the particle electron density. He also observed later a broadening and damping of the SPR absorption band with increasing T in silver nanoparticles about 15 nm in diameter, but with almost no change in the SPR maximum frequency.[43] Some of these features were recorded as well in the low temperature range by Kreibig and Heilmann:[44,45] Decreasing T from ambient temperature to 1.4 K leads to the enhancement and very weak blueshift of the SPR absorption band in the case of gold, silver and copper nanoparticles embedded in gelatin or plasma polymer. Link and El-Sayed also observed a decrease and slight broadening of the SPR band of colloidal gold (22 nm diameter) with increasing T from 18 °C to 72 °C, with no detectable shift within this temperature range.[46]

Chiang *et al.* already attempted to simulate the evolution of the nanocomposite refraction and extinction coefficients by using Maxwell-Garnett and Bruggeman approaches.[17] In this work, the only influence of the electron-electron and electron-phonon scattering variation with temperature on the metallic particle optical properties was accounted. Such a model is obviously not sufficient since it predicts an absorption increase with T whatever photon energy, whereas both experiments[42–46] and the present investigation show a decrease in the SPR spectral domain. Following Chiang and coworkers, Gao and Li carried out calculations of the linear and nonlinear optical properties of nanocomposite media as a function of T, in the framework of the Maxwell-Garnett model treated in the spectral representation.[18] In addition to the temperature dependence of the electron-electron and electron-phonon collision parameter γ, the temperature dependence of the electron density involved in the volume plasma frequency was included. Authors found for Au:MgF_2 that linear absorption decrease (resp. increase) with increasing T for photon energies lower (greater) than 5.0 eV, while the energy of the SPR band maximum does not vary. Liz-Marzán and Mulvaney carried out measurements of the evolution of the SPR absorption band in gold colloidal aqueous and ethanolic solutions (the gold nanoparticles are coated with a silica shell) within the temperature ranges 14–70 °C and 16–50 °C, respectively.[19] They observed no significant shift but a damping of the SPR band with increasing T. Analyzing their results through the Drude description of the metal optical properties, they came to the conclusion that thermally-induced changes of both solvent density and conduction electron scattering frequency are the main mechanisms involved, whereas metal volume thermal expansion and temperature dependence of the solvent refraction index are negligible. They also inferred that the influence of the surrounding medium thermal expansion may be much reduced for nanoparticles embedded in a solid dielectric matrix.[19]

All these theoretical approaches account for the thermally-induced change of the quasifree electron behavior through the Drude description of their contribution to the metal dielectric function. Our approach is somehow different, as we have extracted the complex thermo-optical coefficient of bulk gold from results of the literature, which implicitly includes the influence of both quasifree electrons and interband transitions. We then have determined the effective thermo-optical response of the nanocomposite material by

deriving the Maxwell-Garnett model, including also the temperature dependence of metal concentration and matrix refractive index.

We have chosen the experimental results of Doremus, reported in Ref. 42, regarding gold particles with a mean radius $R=6$ nm, for evaluating our model; indeed, the experimental temperature range is large, providing significant changes in the optical response, and falls within the applicability domain of the bulk gold thermo-optical coefficients that we have extracted (see Sec. II B). Moreover, the particles are large enough to induce only slight finite size effects. These effects can be taken into account in a phenomenological manner by modifying the collision parameter, γ, of the Drude theory for the intraband contribution to the dielectric function [see Eq. (1)]. Note that such a limitation of the conduction electron mean free path may also stem from the possible increased number of lattice defects in the particles as compared to the bulk. The interband contribution to $\tilde{\varepsilon}$ has been first determined from the experimental dielectric function of gold by following the procedure described in Ref. 47. The Maxwell-Garnett model [Eq. (3)] has then been fitted to the experimental absorption spectrum at ambient temperature reported by Doremus, with p and γ [Eq. (1)] as free parameters. The result is reported in Fig. 6(a) (dotted line), showing the spectral variations of the absorption defined as $\alpha=2n\kappa/\lambda$ (λ is the light wavelength) as in Ref. 42. The agreement between the experimental data and the fitted model curve is very good. The metal concentration is found to be worth 5.3×10^{-5}, which falls within the range reported by Doremus (4×10^{-5} to 8×10^{-5}), and $\gamma=0.23$ eV. The slight discrepancy between the latter and the bulk value of 0.14 eV,[48] stems from different effects leading to the reduction of the electron mean free path (surface scattering due to finite size, lattice defects) as stated above.

The derivative of absorption relative to temperature, $d_T\alpha$, has been extracted from the data of Doremus at 25 °C and 514 °C [solid lines of Fig. 6(a)]. The result is shown on Fig. 6(b) (solid line) together with the corresponding calculated value obtained by using the method described in Sec. III A (dashed line). The metal concentration and the collision factor of the Drude contribution to $\tilde{\varepsilon}$ are those fitted at ambient temperature as described in the preceding paragraph. No additional fit has led to the theoretical results of Fig. 6(b). In these conditions, a rather good qualitative agreement can be observed between experimental and theoretical curves: the order of magnitude of $d_T\alpha$ is well estimated by the model, and the existence of a positive maximum at low photon energy and a negative minimum at the plasmon resonance are predicted. However, several discrepancies can be pointed out: The magnitude of the absorption changes with temperature appears overestimated, the maximum at low energy is shifted to the red as compared with the experimental result, and the sign change at ~2.5 eV as well as the fact that $d_T\alpha$ tends to zero towards UV are not predicted. These discrepancies are thought to stem from the model assumption of a free thermal expansion of the metal particles, which may not be valid in the case of a solid matrix host as already highlighted by transmission electron microscopy and extended x-ray absorption fine structure (EXAFS) experiments.[49,50] The thermal expansion of glass-embedded particles is expected to be reduced as compared to the bulk case, due to constraint at the particle-matrix interface. This was already suggested in the analysis of time-resolved x-ray diffraction in silver and gold nanoparticles[51] (see especially endnote [24] of Ref. 51). If metal thermal expansion is limited as compared to free particles, the change in the dielectric function will be lowered. This may especially be true regarding the contribution of interband transitions, the thermal variations of which are due to the band structure modifications subsequent to lattice parameter changes. In order to assess the assumption of a reduced lattice expansion in glass-embedded nanoparticles, the contribution of metal intrinsic thermo-optical effect, characterized by $d_T\tilde{n}$, to the effective medium thermo-optical coefficients has been arbitrarily divided by a factor three in the present model. Let us recall that the contribution of the concentration change, d_Tp, remains negligible in this spectral range. The results are reported on Fig. 6(b) (dashed line). Apart from the sign inversion at ~2.5 eV, one can observe a much better prediction of the experimental data for $d_T\alpha$, regarding the magnitude of the absorption changes, their spectral location, and their cancellation towards UV. Of course, a more accurate analysis should be required to precisely determine the effect of confinement and strain on the optical and thermo-optical properties of metal nanoparticles.[52] Nevertheless, these results validate the theoretical approach presented above.

IV. CONCLUSION

The thermo-optical properties of composite materials consisting of metal nanoparticles embedded in a dielectric host medium have been calculated and illustrated in the case of $Au:SiO_2$. The calculation lies on the Maxwell-Garnett effective medium model in which the temperature dependence of both dielectric functions and relative filling fractions of metal particles and matrix are taken into account. The striking influence of the local electromagnetic field enhancement in the vicinity of the surface plasmon resonance of the nanoparticles has been demonstrated. Consequently, the thermo-optical response of such nanocomposite media is expected to be very sensitive to any phenomenon or morphological characteristics known to affect the local electromagnetic field enhancement as, for instance, quantum size effects, chemical interface damping, or spatial organization of the particles. These predictions may be confirmed by experiments by using methods similar to those employed earlier for pure metals, such as thermomodulation spectroscopy. Additional mechanisms, as particle finite size effects in both metal dielectric function and metal thermal expansion coefficient, should also be included in order to improve the description of the thermo-optical response of nanocomposite materials.

ACKNOWLEDGMENT

This work is financially supported by the Région Ile-de-France, under the project SESAME E-1751.

*Corresponding author. Email address: bruno.palpant@upmc.fr

[1] L. R. Hirsch, R. J. Stafford, J. A. Bankson, S. R. Sershen, B. Rivera, R. E. Price, J. D. Hazle, N. J. Halas, and J. L. West, Proc. Natl. Acad. Sci. U.S.A. **100**, 13549 (2003).
[2] S. Papernov and A. W. Schmid, J. Appl. Phys. **92**, 5720 (2002).
[3] F. Bonneau, P. Combis, J. L. Rullier, M. Commandré, A. During, J. Y. Natoli, M. J. Pellin, M. R. Savina, E. Cottancin, and M. Pellarin, Appl. Phys. Lett. **83**, 3855 (2003).
[4] R. Carminati and J.-J. Greffet, Phys. Rev. Lett. **82**, 1660 (1999).
[5] V. M. Samsonov and N. Y. Sdobnyakov, Cent. Eur. J. Phys. **1**, 344 (2003).
[6] D. Xie, W. Qi, and M. Wang, Acta Metall. Sinica (China) **40**, 1041 (2004).
[7] G. Domingues, S. Volz, K. Joulain, and J.-J. Greffet, Phys. Rev. Lett. **94**, 085901 (2005).
[8] W. H. Qi, M. P. Wang, M. Zhou, and W. Y. Hu, J. Phys. D **38**, 1429 (2005).
[9] Y. Hamanaka, N. Hayashi, S. Omi, and A. Nakamura, J. Lumin. **76&77**, 221 (1997).
[10] H. Inouye, K. Tanaka, I. Tanahashi, and K. Hirao, Phys. Rev. B **57**, 11334 (1998).
[11] J.-Y. Bigot, V. Halté, J.-C. Merle, and A. Daunois, Chem. Phys. **251**, 181 (2000).
[12] C. Voisin, N. Del Fatti, D. Christofilos, and F. Vallée, J. Phys. Chem. B **105**, 2264 (2001).
[13] H. B. Liao, R. F. Xiao, J. S. Fu, H. Wang, K. S. Wong, and G. K. L. Wong, Opt. Lett. **23**, 388 (1998).
[14] M. Falconieri, J. Opt. A, Pure Appl. Opt. **1**, 662 (1999).
[15] R. A. Ganeev, A. I. Ryasnyansky, A. L. Stepanov, and T. Usmanov, Opt. Quantum Electron. **36**, 949 (2004).
[16] M. Rashidi-Huyeh and B. Palpant, J. Appl. Phys. **96**, 4475 (2004).
[17] H. P. Chiang, P. T. Leung, and W. S. Tse, Solid State Commun. **101**, 45 (1997).
[18] L. Gao and Z. Y. Li, J. Appl. Phys. **91**, 2045 (2002).
[19] L. M. Liz-Marzán and P. Mulvaney, New J. Chem. **22**, 1285 (1998).
[20] B. R. Cooper, H. Ehrenreich, and H. R. Philipp, Phys. Lett. A **138**, A494 (1965).
[21] M. L. Thèye, Phys. Rev. B **2**, 3060 (1970).
[22] S. Kupratakuln, J. Phys. C **3**, 109 (1970).
[23] N. E. Christensen and B. O. Seraphin, Phys. Rev. B **4**, 3321 (1971).
[24] P. B. Johnson and R. W. Christy, Phys. Rev. B **6**, 4370 (1972).
[25] D. E. Aspnes, E. Kinsbron, and D. D. Bacon, Phys. Rev. B **21**, 3290 (1980).
[26] J. Hodgson, J. Phys. Chem. Solids **29**, 2175 (1968).
[27] G. P. Pells and M. Shiga, J. Phys. C **2**, 1835 (1969).
[28] P. Winsemius, F. F. van Kampen, H. P. Lengkeek, and C. G. van Went, J. Phys. F: Met. Phys. **6**, 1583 (1976).
[29] R. Rosei and D. W. Lynch, Phys. Rev. B **5**, 3883 (1972).
[30] R. Rosei, F. Antonangeli and U. M. Grassano, Surf. Sci. **37**, 689 (1973).
[31] M. Guerrisi, P. Winsemius, and R. Rosei, Phys. Rev. B **12**, 557 (1975).
[32] P. Winsemius, M. Guerrisi, and R. Rosei, Phys. Rev. B **12**, 4570 (1975).
[33] R. A. Innes and J. R. Sambles, J. Phys. F: Met. Phys. **17**, 277 (1987).
[34] *Handbook of Optical Constants of Solids*, Vols. I and II, edited by E. D. Palik (Academic Press, New York, 1985/1991).
[35] J. C. Maxwell-Garnett, Philos. Trans. R. Soc. London **203**, 385 (1904).
[36] F. C. Nix and D. MacNair, Phys. Rev. **60**, 597 (1941).
[37] J. W. Berthold III and S. F. Jacobs, Appl. Opt. **15**, 2344 (1976).
[38] M. Medhat, S. Y. El-Zaiat, A. Radi, and M. F. Omar, J. Opt. A, Pure Appl. Opt. **4**, 174 (2002).
[39] S. C. Mehendale, S. R. Mishra, K. S. Bindra, M. Laghate, T. S. Dhami, and K. C. Rustagi, Opt. Commun. **133**, 273 (1997).
[40] R. A. Ganeev, A. I. Ryasnyansky, Sh. R. Kamalov, M. K. Kodirov, and T. Usmanov, J. Phys. D **34**, 1602 (2001).
[41] D. D. Smith, G. Fischer, R. Boyd, and D. A. Gregory, J. Opt. Soc. Am. B **14**, 1625 (1997).
[42] R. H. Doremus, J. Chem. Phys. **40**, 2389 (1964).
[43] R. H. Doremus, J. Chem. Phys. **41**, 3259 (1964); **42**, 414 (1965).
[44] U. Kreibig, J. Phys. (France) **38**, C2 (1977).
[45] A. Heilman and U. Kreibig, Eur. Phys. J.: Appl. Phys. **10**, 193 (2000).
[46] S. Link and M. A. El-Sayed, J. Phys. Chem. B **103**, 4212 (1999).
[47] B. Palpant, B. Prével, J. Lermé, E. Cottancin, M. Pellarin, M. Treilleux, A. Perez, J.-L. Vialle, and M. Broyer, Phys. Rev. B **57**(3), 1963 (1998).
[48] N. W. Ashcroft and N. D. Mermin, *Solid State Physics* (Saunders College, Holt, Rinehardt & Winston, Philadelphia, 1976).
[49] M. Dubiel, S. Brunsch, and L. Tröger, J. Phys.: Condens. Matter **12**, 4775 (2000).
[50] M. Dubiel, S. Brunsch, W. Seifert, H. Hofmeister, and G. L. Tan, Eur. Phys. J. D **16**, 229 (2001).
[51] A. Plech, S. Kürbitz, K.-J. Berg, H. Graener, G. Berg, S. Grésillon, M. Kaempfe, J. Feldmann, M. Wulff, and G. von Plessen, Europhys. Lett. **61**, 762 (2003).
[52] U. Gerhardt, Phys. Rev. **172**, 651 (1968).